Electronic Supplementary Material (ESI) for ChemComm.

Supporting Information

Increasing the selectivity to ethylene in MTO reaction by enhancing diffusion limitation in the shell layer of SAPO-34 catalyst

Jiawei Zhong, Jingfeng Han, Yingxu Wei,* Shutao Xu, Yanli He, Mao Ye, Xinwen Guo, Chunshan Song, Zhongmin Liu*

Experiment

Catalyst Preparation

H-SAPO-34 was exchanged with 1 M NH_4NO_3 solution twice with liquid-to-solid (L/S) ratio of 10 mL/g at 80 ^oC for 2 h, which was followed by a filtration, washing and drying procedure. The NH_4-SAPO-34 was exchanged with 0.01 M $Zn((NO_3)_2.6H_2O$ solution with L/S ratio of 30 mL/g at 50 ^oC for 4 h, which was followed by filtration, washing and drying procedure. The powder was calcined at 550 ^oC for 4 h. The obtained SAPO-34 with zinc cation modification is denoted as Zn-SAPO-34.

For comparison, H-SAPO-34 was exchanged with 1M NH_4NO_3 solution twice with liquid-to-solid (L/S) ratio of 10 mL/g at 80 ^oC for 2 h, which was followed by a filtration, washing and drying procedure. The NH_4-SAPO-34 was impregnated with $Zn((NO_3)_2.6H_2O$ solution at room temperature with the theoretical amount of 0.4wt%. The powder was dried and calcined at 550 ^oC for 4 h.[1] The obtained SAPO-34 with zinc oxide modification is denoted as Zn-SAPO-34-IMP.

Catalyst Characterization

The X-ray diffraction (XRD) was conducted on PANalytical X'Pert PRO X-ray diffractometer. Cu Kα radiation (λ = 1.54059 Å) was used as the X-ray source, operated at 40 mA and 40 kV. XRD patterns were recorded in the range of $2\theta = 5\text{-}40^o$.

X-ray fluorescence (XRF) was conducted with Philips Magix-601 spectrometer.

The nitrogen adsorption-desorption was conducted with Micromeritics ASAP 2020 at -196 ^oC after the sample was degassed at 350 ^oC under vacuum. The total surface area was calculated according to the BET equation. The micropore volume, external surface area and micropore surface area were calculated by the t-plot method. The total pore volume was determined from the amount adsorbed at the relative pressure of 0.99.

Diffuse reflectance infrared Fourier-transform spectra (DRIFTS) were measured on an FT-IR spectrometer (Tensor 27, Bruker). The catalysts were heated at 500 ^oC for 0.5 h to remove the adsorbed water before each measurement. The DRIFT spectra were recorded in the range of 4000–600 cm^{-1} with a resolution of 4 cm^{-1}. The spectrum of KBr under the same condition was used as the background.

The solid-state NMR spectroscopy experiments were carried out on a Bruker Avance III 600 spectrometer equipped with a 14.1 T wide-bore magnet using a 4 mm H-X magic angle spinning (MAS) probe. For ^1H MAS NMR spectra, the samples were dehydrated at 400 ℃ for 20 h at a pressure of less than 10^{-3} Pa. The resonance frequencies were 600.13 MHz. Chemical shifts were referenced to admantane at 1.74 ppm.

Temperature-programmed reduction by H_2 (H_2-TPR) measurements was performed with Micromeritics Autochem II 2920. The samples were pre-treated at 550 ^oC for 60 min in Ar. The TPR procedure was conducted from 50 to 900 ^oC under 10% H_2/Ar. The consumption of H_2 was detected by TCD.

X-ray photoelectron spectroscopy (XPS) was conducted with Thermo ESCALAB 250Xi. The X-ray excitation was provided by a monochromatic Al Kα source (1486.6 eV, 15 kV, 10.8 mA). Binding energy (BE) values were referenced to the C 1s line of residual carbon at 284.8 eV. The atomic ratio was calculated using the peak areas of Si2p, Al2p, P2p and Zn2p, respectively. Prior to the XPS measurements, the powders were pressed into disks with a diameter of 5 mm. Data analysis was performed using Casa XPS software.

Scanning electron microscopy (SEM) was conduct with Hitachi TM3000 operated at an acceleration voltage of 15 kV. The sample was attached onto conductive double side carbon tapes. The crystal size distribution was calculated with software Nano Measurer.

Energy-dispersive X-ray spectroscopy (EDS) was conducted with cold field emission SEM Hitachi SU8020 equipped with a Horiba X-max silicon drift X-ray detector operated at an acceleration voltage of 20 kV.

Diffusion Properties

The adsorption isotherms of ethane, propane and n-butane were performed on a gravimetric analyser (IGA100, Hiden Isochema Ltd., Warrington, UK). A sensitive microbalance (resolution of 0.1 μg) was mounted in a thermostatted enclosure to remove thermal coefficients of the weighing system and provide a high stability and accuracy. Typically, about 100 mg samples were loaded into the microbalance bucket and outgassed under a vacuum less than 10^{-3} Pa at 400 ^oC for more than 10 h prior to the sorption measurements. The sample temperature was regulated within 0.1 K by a furnace. The adsorption isotherms were obtained at 20 ℃ and the pressure was determined by two high accuracy Baratron pressure transducers. For each step, the amount of sorbate (ethane >99.99% purity, propane >99.8% purity, n-butane >99.8% purity) introduced into the system was kept low enough to keep the adsorption process isothermal. The dosing continued until the entire equilibrium adsorption isotherm was obtained. The adsorption kinetics curve of ethane, propane and n-butane was recorded at a pressure of 10 mba.

Ethylene or propylene diffusion in the catalyst bed of SAPO-34 and Zn-SAPO-34 were evaluated with chromatographic method. The sample was heated from room temperature to 500 ^{o}C under helium for 0.5 h. Pulses containing ethylene or propylene (Ethylene 4.87%, propylene 4.89%, He as the balance gas) were respectively injected to catalyst bed for 0.6 second by switching a four-port valve, and the concentration of probe molecules (C(t)) escaping from the catalyst bed was detected by Pfeiffer Omnistar GSD 301 T3 Quadrapole Mass Spectrometer Gas Analyzer.

MTO Reaction Test

Typically, the catalyst (1000 mg, 40-60 mesh) was loaded in the tubular quartz fixed-bed reactor at atmospheric pressure and activated under an Ar flow at 550 ^{o}C for 60min, and then the temperature was adjusted to a reaction temperature of 475 °C. A methanol solution with a CH_3OH/H_2O weight ratio of 40/60 was consequently pumped into the reactor with liquid pump (LC-05P), corresponding to the weight hourly space velocity (WHSV) of 2.0 h^{-1}. The composition of the exit gas was analysed by online gas chromatograph (Agilent GC 7890A) using flame ionization detector (FID) with capillary column CP-PoraPlot Q-HT (25m * 0.32mm * 20um) and thermal conductivity detector (TCD) with packed column Porapak QS (3m × 2mm). Hydrocarbons were analysed by FID, while CO, CH_4 and CO_2 were analysed by TCD. CH_4 was taken as a reference bridge between FID signals and TCD signals. The temperature of the effluent line was maintained at 170 °C by heating belt to ensure the products in gas phase. Conversions and selectivities were computed on a carbon mole basis, reported selectivities are normalized by the total selectivity of the products observed, and dimethyl ether in the effluent is considered as a reactant.

Analysis of Retained Organics

The retained organics in the catalysts after reaction were analysed with GC-MS. The catalysts were dissolved in 20% HF solution in a screwcap Teflon vial, the organic compounds were extracted with CH_2Cl_2 and analysed by an Agilent 7890A Gas Chromatograph equipped with an Agilent 5795C Mass Selective Detector with a HP-5 capillary column (30 m, 0.25 mm i.d., stationary phase thickness 0.25 um) and an FID detector. The structures annotated onto the chromatograms are peak identifications reference to NIST database. The amount of hydrocarbon compounds was normalized with C_2Cl_6 as the internal standard.

Thermo-gravimetric analysis (TGA) and differential thermogravimetric (DTG) with SDT Q 600 was used to measure the coke removal. The sample was heated from room temperature to 900 °C at a rate of 10 °C/min under flowing air (100 mL/min). And catalysts after methanol reaction at 475 °C for 2 min was kept isothermal in 150 °C for additional 30min for complete removal of adsorbed water

Results

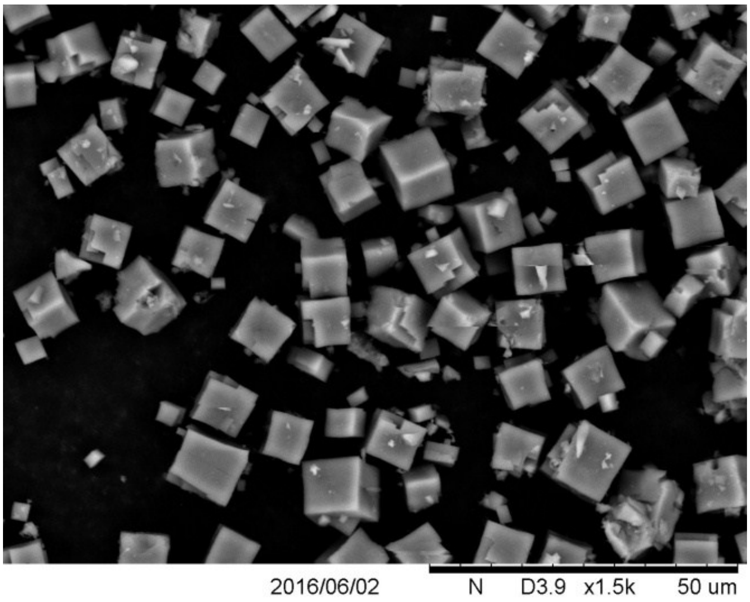

Fig. S1 The SEM image of H-SAPO-34

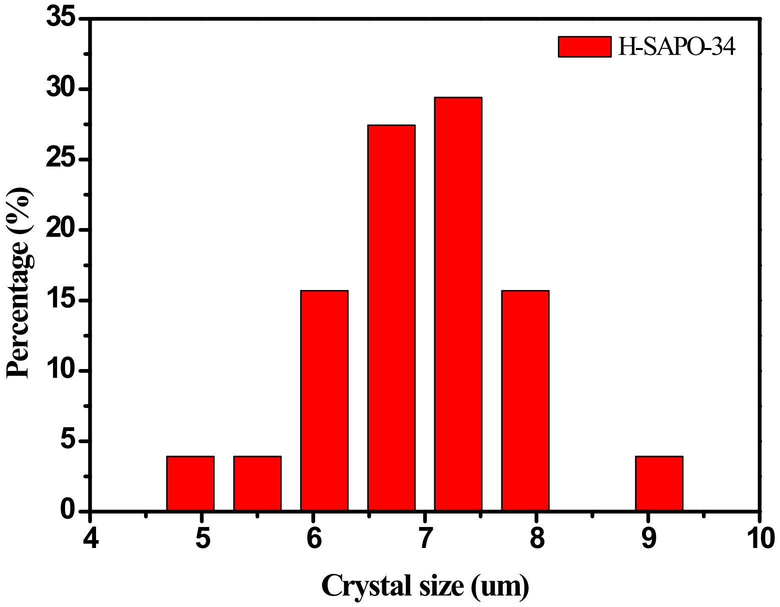

Fig. S2 The particle distribution of H-SAPO-34

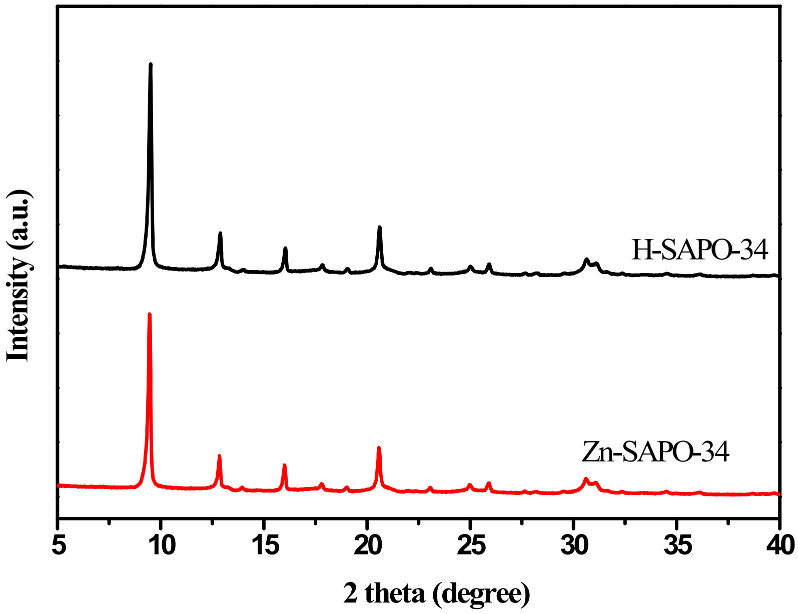

Fig. S3 XRD patterns of H-SAPO-34 and Zn-SAPO-34

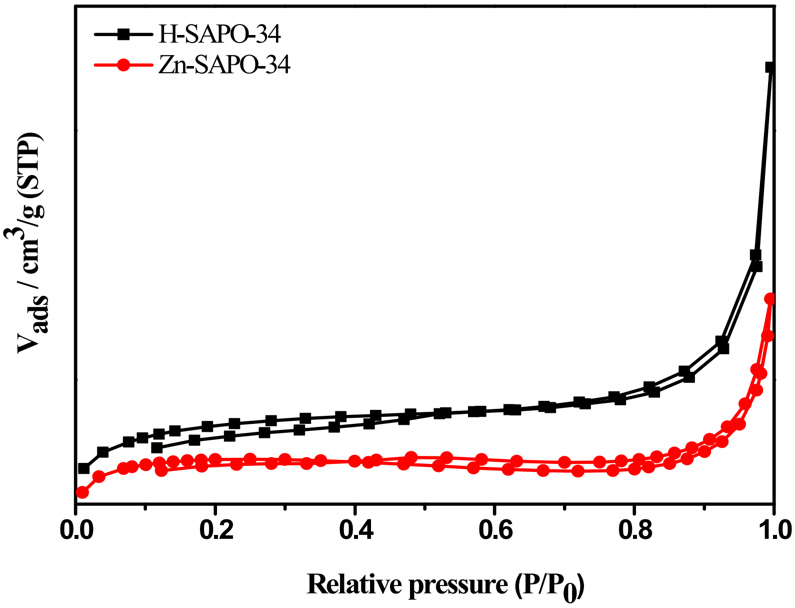

Fig. S4 Nitrogen adsorption/desorption isotherms of H-SAPO-34 and Zn-SAPO-34

Table S1. Textual properties of H-SAPO-34 and Zn-SAPO-34

Sample	Surface area (m^2/g)			Pore Volume (cm^3/g)	
	S_{total} [a]	S_{micro} [b]	S_{ext} [c]	V_{total}	V_{micro} [d]
H-SAPO-34	471.2	462.6	8.6	0.24	0.22
Zn-SAPO-34	462.2	458.1	4.1	0.23	0.21

a: BET surface area; b: t-plot micropore surface area; c: t-plot external surface area; d: t-plot micropore volume

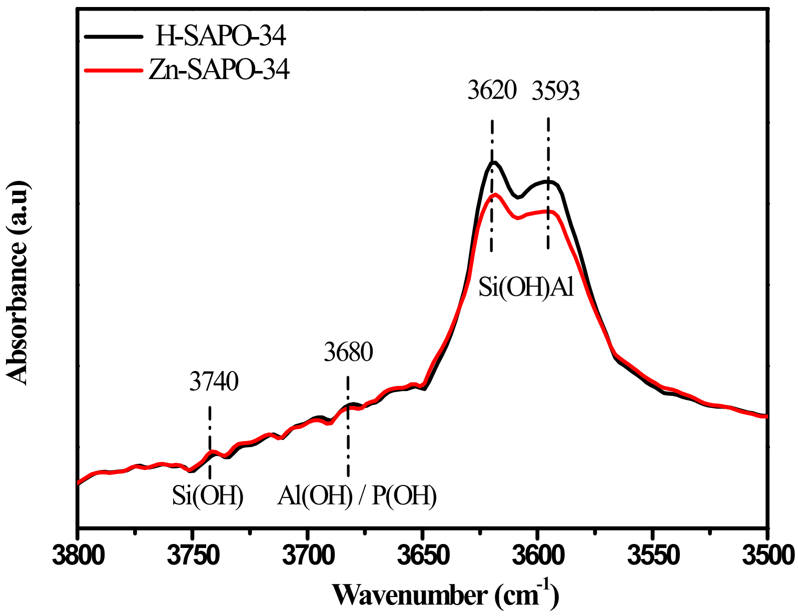

Fig. S5 The FTIR spectra of H-SAPO-34 and Zn-SAPO-34

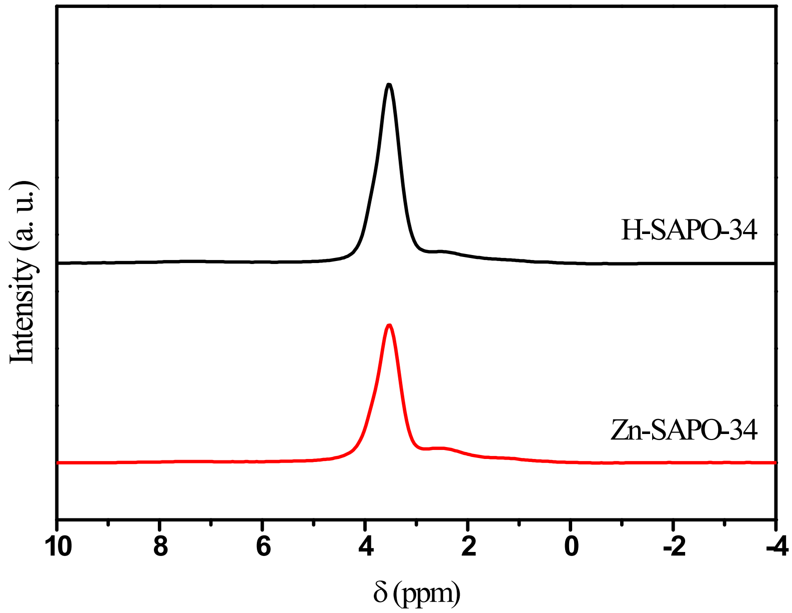

Fig. S6 ^{1}H MAS NMR spectra of the H-SAPO-34 and Zn-SAPO-34

Table S2. Density of Si(OH)Al of H-SAPO-34 and Zn-SAPO-34

	Sample	
	H-SAPO-34	Zn-SAPO-34
Density of Si(OH)Al (mmol/g)	0.9	0.8

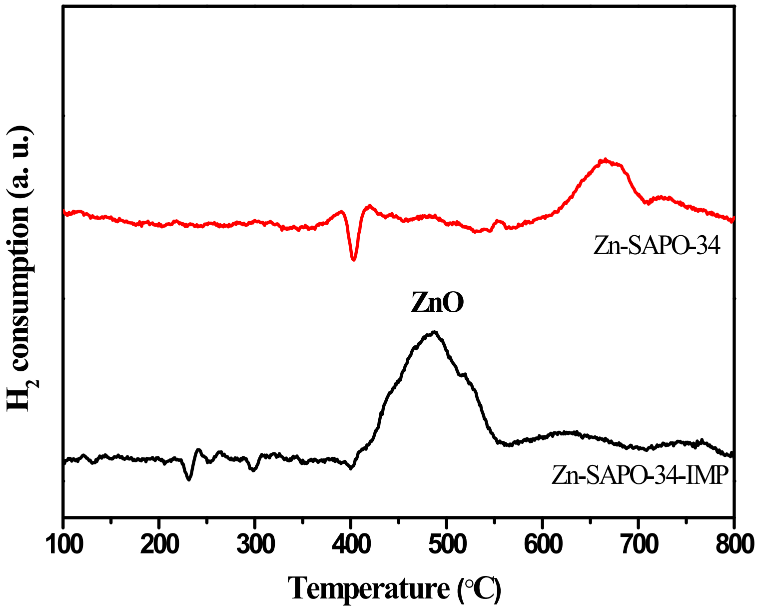

Fig. S7 H_2-TPR profiles of Zn-SAPO-34 and Zn-SAPO-34-IMP

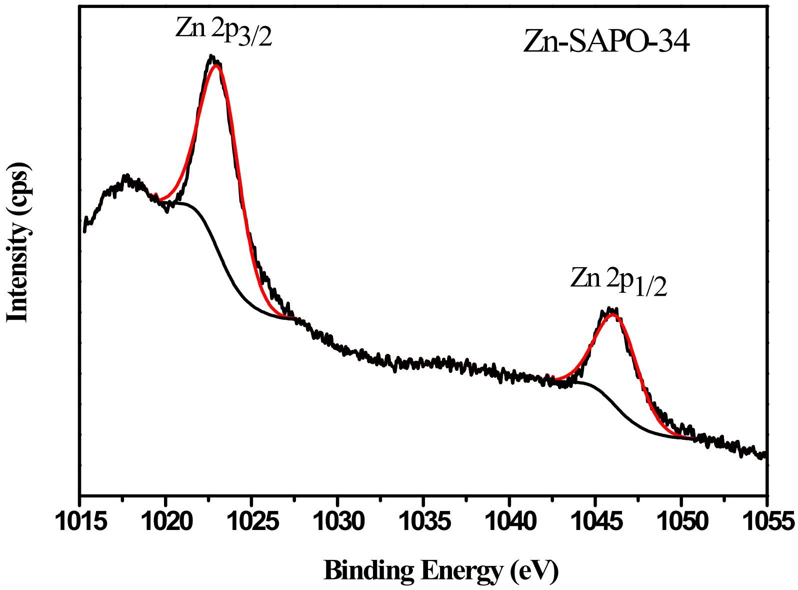

Fig. S8 Zn 2p XPS core level spectra for Zn-SAPO-34

Table S3 The composition and metal dispersion in Zn-SAPO-34.

Elemental composition of SAPO-34 (mol %)	Bulk [a]	$Si_{0.085}Al_{0.490}P_{0.425}$
	Surface [b]	$Si_{0.100}Al_{0.480}P_{0.420}$
	R_{Si} [c]	1.2
Zn content in Zn-SAPO-34 (wt %)	Bulk [a]	0.34
	Surface [b]	0.70
	R_{Zn} [c]	2.1

a: Determined by XRF.

b: Determined by XPS.

c: The surface Si(Zn) enrichment index R_{Si} or R_{Zn} is de-fined as $[Si/(Si + P + Al)]_{surface}/[Si/(Si + P + Al)]_{bulk}$, and $Zn_{surface} / Zn_{bulk}$

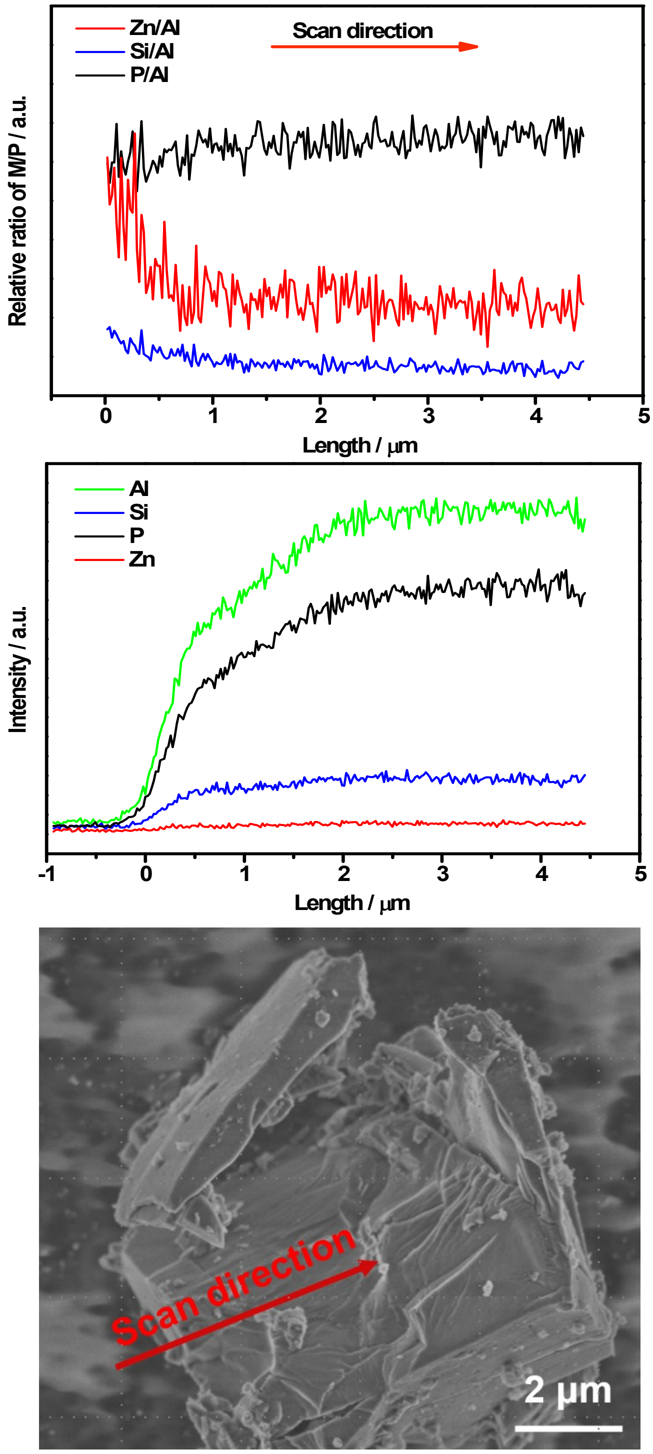

Fig. S9 The EDX analysis along the scan direction marked in red in the SEM image of Zn-SAPO-34

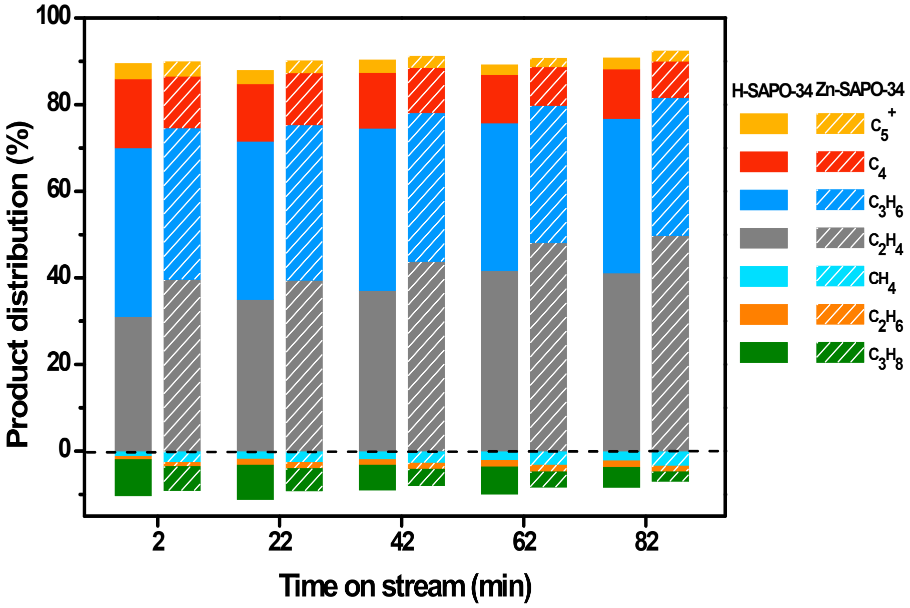

Fig. S10 The product distribution of methanol conversion over H-SAPO-34 and Zn-SAPO-34.

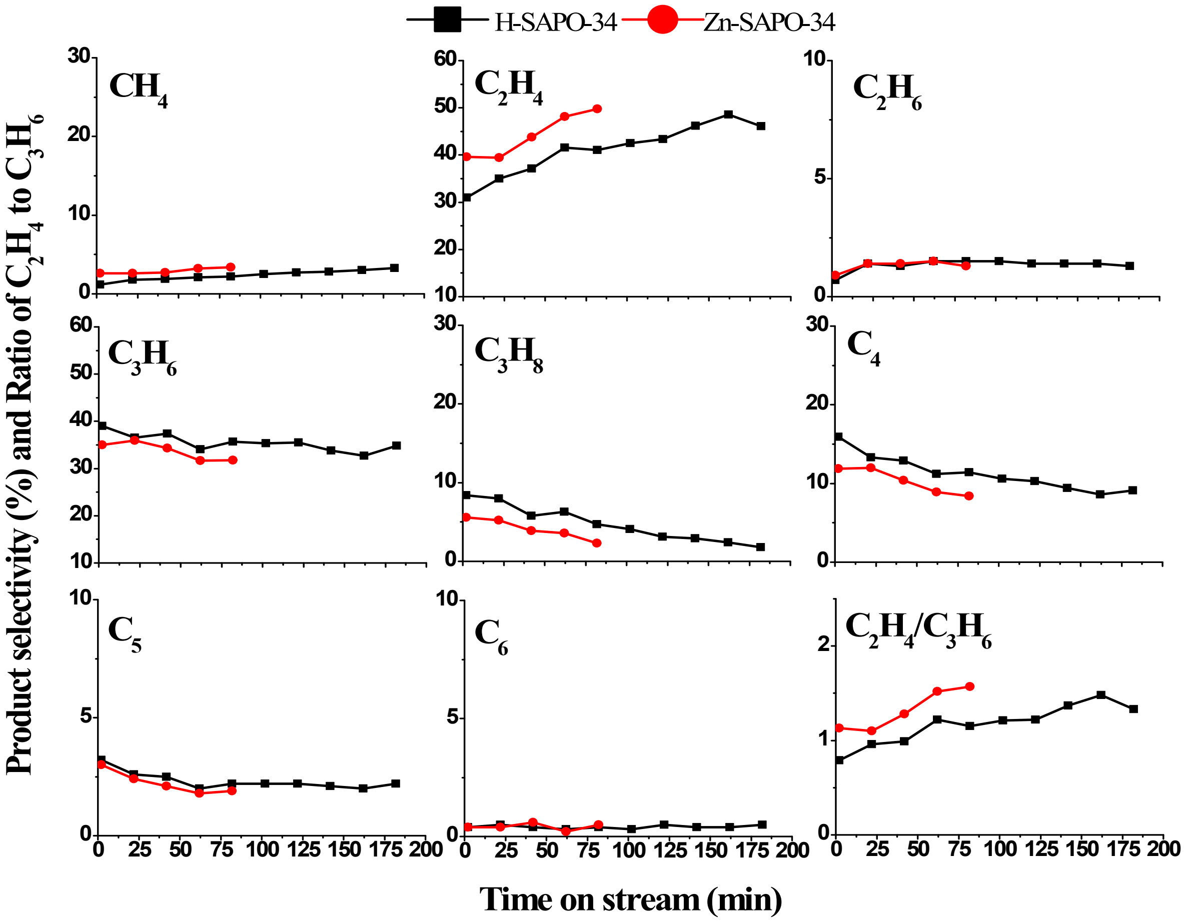

Fig. S11 The products distribution and ratio of C_2H_4 to C_3H_6 of MTO reaction over H-SAPO-34 and Zn-SAPO-34

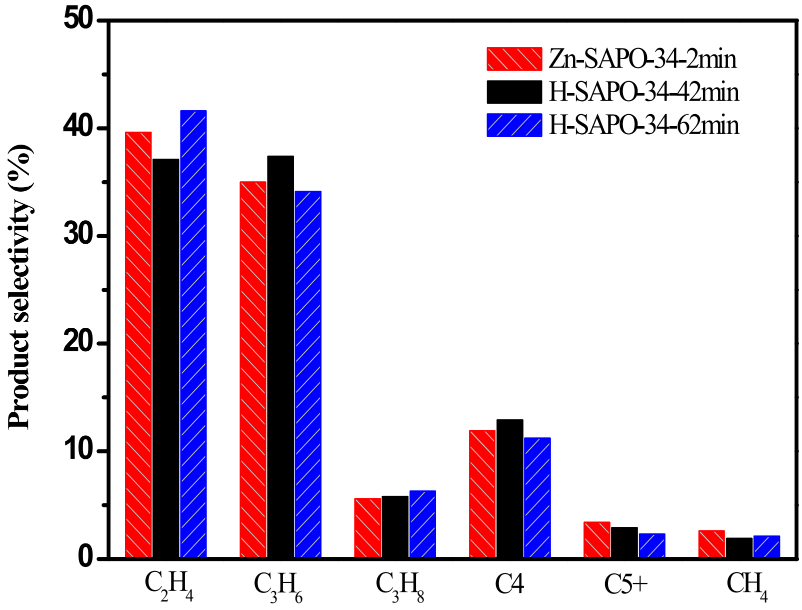

Fig. S12 The product distribution over Zn-SAPO-34-2min, H-SAPO-34-42min and H-SAPO-34-62min

Table S4 The products distribution of MTO reaction over H-SAPO-34 and Zn-SAPO-34 (TOS=2 min)

Product Distribution (%)	CH_4	C_2H_4	C_2H_6	C_3H_6	C_3H_8	C4	C5	C6	CO	CO_2
Zn-SAPO-34	2.6	39.7	0.9	35.1	5.6	11.9	3.0	0.4	0.4	0.5
H-SAPO-34	1.2	31.0	0.7	39.0	8.5	15.9	3.3	0.4	0.1	0

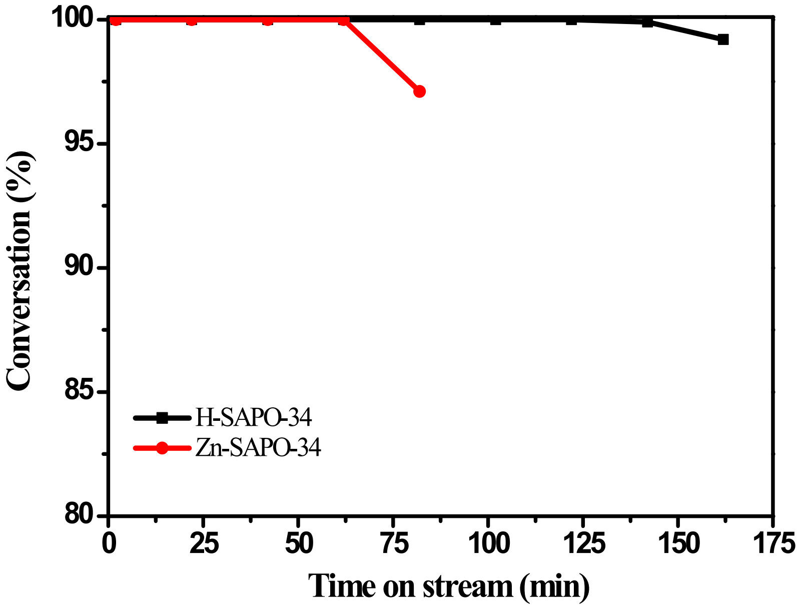

Fig. S13 Methanol conversion over H-SAPO-34 and Zn-SAPO-34

$$\frac{\partial C}{\partial t} = D\frac{\partial^2 C}{\partial x^2}$$

$$\frac{q(t)}{q(m)} = \frac{6}{\sqrt{\pi}}\sqrt{\frac{D}{r^2}}\sqrt{t}$$

Eq. S1 Fick's second law and the derived equation:

[q(t)/q(m): normalized loading, D: diffusivity, r: characteristic diffusion length, t: time].[2]

Table S5 The diffusivity (D) of ethane, propane and n-butane over H-SAPO-34 and Zn-SAPO-34 under 10 mba

Sample	H-SAPO-34	Zn-SAPO-34
C_2H_6	2.30×10^{-14}	1.44×10^{-14}
C_3H_8	1.62×10^{-15}	9.98×10^{-16}
n-C_4H_{10}	8.29×10^{-16}	6.29×10^{-16}

Table S6 The diffusivity (D) of ethane over H-SAPO-34 and Zn-SAPO-34 under 10 mba

Sample	D $\times10^{14}$/ (m^2/s)
H-SAPO-34	2.30
Zn-SAPO-34	1.44
H-SAPO-34-2min	1.76
Zn-SAPO-34-2min	1.34
H-SAPO-34-42min	0.694

$$E(t) = \frac{C(t)}{\int_0^\infty C(t)dt}$$

Eq S2. Residence time distribution (RTD)

[C(t): concentration of probe molecules exiting the catalyst bed, t: time]

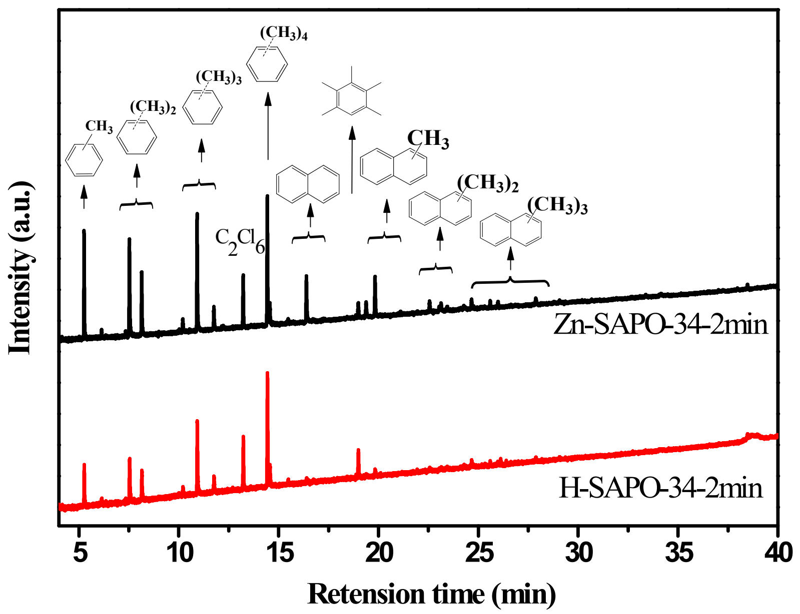

Fig. S14 GC-MS chromatograms of hydrocarbon compounds at 475 °C after 2 min retained in H-SAPO-34 and Zn-SAPO-34.

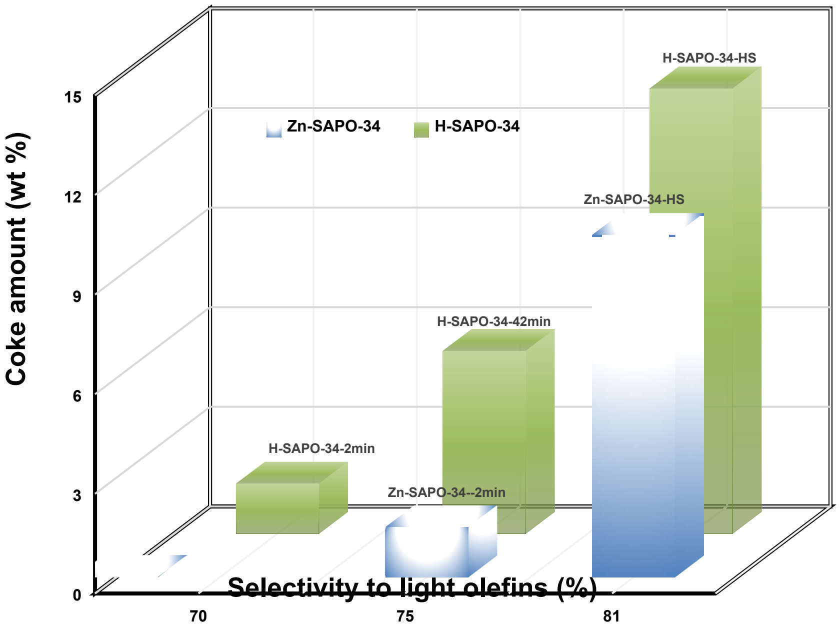

Fig. S15 The relationship between coke amount and selectivity to light olefins over H-SAPO-34 and Zn-SAPO-34.

1. Wang, J.; Huang, Y.; Yu, T.; Zhu, S.; Shen, M.; Li, W.; Wang, J. *Catal. Sci. Tech.* **2014,** *4* (9), 3004.
2. Zheng, J.; Zeng, Q.; Zhang, Y.; Wang, Y.; Ma, J.; Zhang, X.; Sun, W.; Li, R. *Chem. Mater.* **2010,** *22* (22), 6065-6074.